Available online at www.sciencedirect.com
SCIENCE DIRECT
Separation and Purification Technology 44 (2005) 250–257
Separation and Purification Technology
www.elsevier.com/locate/seppur

Cake layer morphology in microfiltration of activated sludge wastewater based on fractal analysis

F.G. Meng *, H.M. Zhang, Y.S. Li, X.W. Zhang, F.L. Yang, J.N. Xiao

School of Environmental and Biological Science and Technology, Dalian University of Technology, Dalian 116024, PR China

Received 21 August 2004; received in revised form 17 January 2005; accepted 27 January 2005

Abstract

Membrane bioreactor (MBR) is an important solid–liquid separation technology employed widely in the wastewater treatment. However, membrane permeability decline rapidly due to membrane fouling, which limited the application of MBR. In order to obtain understanding of the complex membrane fouling mechanisms, analysis of the effect of the microstructure on the cake permeability is necessary. In this regard, study of the distribution and porosity of the cake is very necessary. The pore distribution is strongly influenced by cake compressibility but information on how to describe this effect is very limited. In this paper, fractal theory was used to gain knowledge of cake microstructure and its correlation to macroscopic cake properties. Scanning electron microscopy (SEM) and image analysis were utilized to estimate pore size and pore size distributions. The two-dimensional fractal dimension was determined. The results show that the cake layer had a good fractal characteristic, and the fractal dimension (D_s) was linearly correlated with porosity ($R^2 = 0.929$). The fractal dimension had some relation with cake resistance and cake specific resistance. It indicates that fractal dimension provides an approach for quantification of cake structure and cake permeability.

Keywords: Membrane bioreactor; Membrane fouling; Cake layer structure; Cake permeability; Fractal theory

1. Introduction

In recent years, membrane bioreactors (MBRs) have been widely used in wastewater treatment to achieve higher effluent quality, which is often difficult to be effectively met by conventional activated sludge process. The advantages of MBRs are a high mixed liquor suspended solids (MLSS) concentration, up to 35 g/L, producing higher rate of removal of BOD and COD, a lower excess sludge production and the production of treated water can be reused [1]. In addition, the space occupied by MBRs system is greatly reduced due to the absence of settling tanks and the reduction in bioreactor volume made possible by the higher biomass concentration. But a major obstacle for the application of MBRs is the rapid decline of the permeation flux as a result of membrane fouling. That is to say, membrane fouling in MBRs reduces productivity and increases maintenance and operation costs. Thus, membrane fouling is the key problem to be resolved.

In general, membrane fouling is attributed to initial pore blocking followed by cake formation. As an example, Lee et al. reported that membrane resistance, cake resistance, pore blocking and irreversible fouling resistance contributed 12, 80, and 8%, respectively to the total resistance of a submerged MBR [2]. The formation of the microfiltration cake layer is a dynamic process, which can be divided into the three stages: pore blocking at the beginning of filtration, cake formation, and cake compression [3,4]. In the second and the third stage, there are a rapid increase in filtration resistance and a decrease in cake porosity due to cake compression [5]. Therefore, analysis of the filter cake formation mechanism is an effective approach to control membrane fouling. The cake layer on the membrane surface has been found to be microstructure, including its surface and cross-section [6,7]. And microstructure of the fouling layer influences membrane permeation.

* Corresponding author. Tel.: +86 411 84706172; fax: +86 411 84708040.
E-mail address: fgmeng80@126.com (F.G. Meng).

1383-5866/$ – see front matter © 2005 Elsevier B.V. All rights reserved.
doi:10.1016/j.seppur.2005.01.015

Nomenclature

a_i	pore area (μm^2)
A_i	total area of the pores that equal or larger than a_i (μm^2)
B_i	surplus area (μm^2)
C_0	constant
D_s	fractal dimension
J	permeate flux (L/m^2 h)
L	length scale (m)
$M(L)$	measure of an object with a length of L
r	size of a pore (μm)
r_c	cake specific resistance per unit cake thickness (m^{-2})
r_{max}	size of the largest pore (μm)
R_c	cake layer resistance (m^{-1})
R_m	intrinsic membrane resistance (m^{-1})
R_p	pore blocking resistance (m^{-1})
R_t	total resistance (m^{-1})
S_c	total area of cake layer analyzed (μm^2)
TMP	transmembrane pressure (Pa)
WHD	water head drop (cm)

Greek letters

δ_c	cake thickness (μm)
φ	porosity (%)
μ	dynamic viscosity (Pa s)

The surface morphology and internal microstructure of cake layer deposited on membrane surface can be studied by such techniques as scanning electron microscopy (SEM), atomic force microscopy (AFM), small-angle neutron scattering (SANS), static light scattering (SLS), etc. [8–10]. Hwang and Hsueh studied the filtration characteristics of Dextran–MnO_2 colloidal aggregates [8]. From cake structure observations using scanning electron microscopy, they concluded that a skin layer may be constructed next to the membrane surface when a certain amount of cake is formed, and that this cake layer was the major source of filtration resistance. Su et al. utilized SANS to carry out in situ studies of membrane pore blockage during ultrafiltration of protein solutions by alumina membranes [9]. Hamachi et al. analyzed the bentonite deposit thickness by means of direct measurement [10]. The principle of the measurement was based on the tangential focusing of a He-Ne laser beam onto the membrane surface. The build-up of a deposit on the membrane surface was expressed as absorption of light, and this variation in signal intensity corresponded directly to the deposit thickness through a calibration curve recorded at the beginning of the experiment. Pignon et al. presented SLS, SANS and local birefringence techniques to quantify the inner structure of deposited colloid fouling layers on the membrane surface [11]. In SLS and SANS, incident light or neutrons were directed through the cake layer resulting in scattering through the deposit. The scattering intensity was then related to the fractal dimension of the deposit.

Numerous studies have been carried out about membrane filtration characteristics or membrane fouling, but most of them focused on cake macro-analysis. Microstructure of cake layer, including volume fraction of the pores, relative location of the pores, geometrical structure of the pores, has not been explored until now, which is a key factor determining membrane permeate flux. The filter cake layer consists of numerous irregular pores of different size spanning several orders of magnitude in length scales. The traditional geometry theory cannot give us a good understanding about it. Fractal theory is a new tool for analysis natural phenomenon, which allows the characterization of objects in terms of their self-similar (scale-invariant) properties (i.e. parts of the object are similar to the whole after rescaling).

Fractal theory has been used in deep bed filtration [12–14]. Kaye investigated the cake filtration mechanism and found cake morphology can be characterized by a fractal geometry image: Seiepinski carpet. Fractal dimension of the cake structure may vary as function of operating condition. The cake layer formed on the membrane surface is very similar to deep filtration cake. Thus, fractal geometry offers a new approach helping us recognize and resolve membrane fouling.

In order to get a better understanding of membrane fouling mechanism, we concentrate our attention on the analysis of membrane fouling cake layer of MBR from the viewpoint of fractal theory. The structure of the cake layer was examined with a scanning electron microscopy and an image analyzer. Some cake layer property parameters and microstructure characteristics were analyzed.

2. Fractal dimension model for cake layer

2.1. Fractal theory

Euclidean geometry describes regular objects such as points, curves, surfaces, and cubes using integer dimensions 0, 1, 2 and 3, respectively. Associated with each dimension is a measure of the object such as the length of a line, area of a surface and volume of a cube. However, numerous natural objects such as coastlines, rivers, lakes, porous media, are disordered and irregular, which cannot be described by Euclidean geometry due to the scale-dependent measures of length, area and volume. These objects are called fractals, and their dimensions are non-integral and defined as fractal dimensions. A fractal object can be divided into parts, each of which is similar with the whole.

For example, the length of a coastline of a country would depend on the size of the measuring stick used; decreasing the length of the measuring stick leads to a better resolution of the convolutions of the coastline, and as the length of the stick approaches zero, the coastline's length approaches infinity. This is the fractal nature of the coastline. The measure of a

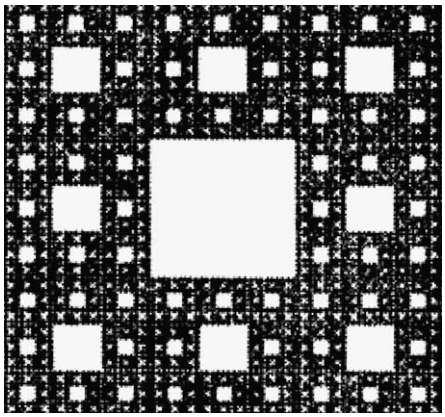

Fig. 1. A famous fractal image: Sierpinski carpet.

fractal object, $M(L)$, is related to the length scale, L, following the scaling law in the form of:

$$M(L) \sim L^{D_s} \tag{1}$$

Eq. (1) implies the property of self-similarity, which means that the value calculated from Eq. (1) remains constant over a range of length scales, L. The geometry structures such as Sierpinski gasket, Sierpinski carpet (Fig. 1) and Koch curve are the examples of the exact self-similar fractals, which exhibit the self-similarity over an infinite range of length scales [15]. However, self-similarity in a global sense is seldom observed in actual applications. Numerous objects found in nature are not exactly self-similarity, but statistical self-similarity, which implies that these objects exhibit the self-similarity in some average sense and over a certain local range of length scales, L.

2.2. Fractal dimension model for filtration cake layer analysis

Kye et al. developed a Sierpinski fractal model, which is a useful tool to analysis cake pore area distribution and its permeability [13,16–18]. The model can be described as:

$$B(\geq r) = S_c - \int_r^{r_{max}} f(r)\pi r^2 \, dr = C_0(\pi r^2)^{2-D_s} \tag{2}$$

where S_c is the total cake layer area analyzed, $f(r)$ is radii distribution function of cake layer pores, r is the size of a pore, r_{max} is the size of the biggest pore, B is the area of the cake layer subtracted all the area of the pores which size larger than r, defined as surplus area, C_0 is a constant, the fractal dimension, D_s, represents the pore area distribution of the cake layer. The calculation procedure of D_s was as follows:

(i) Evaluate each pore area using an image analyser.
(ii) Define several different area levels/thresholds, a_i, for all the pores.

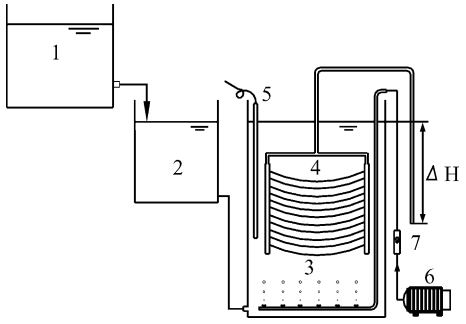

Fig. 2. Schematic of the membrane bioreactor: (1) feed tank; (2) balance box; (3) bioreactor; (4) membrane module; (5) electric heater; (6) air pump; (7) air flow meter.

(iii) Sum all the pores which are equal or larger than a_i, and defined as:

$$A_i = \sum_i a_i \tag{3}$$

(iv) According to Eqs. (2) and (3), a new model will be developed:

$$B_i(\geq a_i) = S_c - A_i = C_0 a_i^{2-D_s} \tag{4}$$

Thus a Richardson plot of $\ln B_i$ versus $\ln a_i$ yields a straight line of slope 2-D_s, enabling the fractal dimension, D_s, of the cake surface to be determined.

3. Experimental procedures

3.1. Membrane bioreactor

As shown in Fig. 2, the experimental system basically consisted of an activated sludge bioreactor in which a membrane module was submerged. The effective volume of the bioreactor was 12 L. The bioreactor was aerated at a flow rate of 0.2 m^3/h. Table 1 shows the specifications of the hollow fiber membranes used in this work. The mixed liquor suspended solids for bioreactor was maintained at about 3000 mg/L (±100 mg/L). The major nutrient sources in feed water to the MBR process were similar with municipal wastewater. The composition of the feed water is listed in Table 2. Sucrose and urea were used as the main nutrition for activated sludge, and dipotassium hydrogen phosphate (K_2HPO_3) and calcium

Table 1
Specifications of the hollow fiber membranes used in the microfiltration study

Membrane material	PE
Nominal pore size (μm)	0.1
Fiber length (mm)	160
External diameter (mm)	0.370
Internal diameter (mm)	0.270
No. of membranes in module	600
Total membrane surface area (m^2)	0.11
R_m (m^{-1})	1.05×10^{-11}

Table 2
Composition of feed water

Composition	Concentration (mg/L)
Sucrose	300
Urea	78
$CaCl_2$	5
K_2HPO_3	38
$NaHCO_3$	40

chloride ($CaCl_2$) were applied as microelements. Sodium bicarbonate ($NaHCO_3$) was used as a buffer to adjust the mixed liquor pH to about 7.0. The temperature of the mixed liquor was maintained at 25.0 °C with an electric heater.

3.2. Typical experimental procedure

3.2.1. Microfiltration experiments

During the operation of microfiltration, the membrane module was driven by a fixed water head drop (WHD). And the membrane filtration was continuously operated to gain a steady cake layer as soon as possible. Three WHDs were adopted to examine the filtration cake morphology with different TMP. Each membrane filtration cycle was maintained at 24 h, and the volume of the bioreactor was constant at 12 L with a balance box (see Fig. 2), so the feed water was continuous provided by the feed tank. To ensure that the condition and performance of the membrane module was almost the same in all experiments, post-cleaning was performed after every experiment to remove the fouling cake. In membrane filtration process, permeate rate was measured to compare microfiltration performance of different TMP.

3.2.2. Microfiltration resistance analysis

Membrane resistance is defined by the Darcy's law as follows:

$$R_t = R_m + R_p + R_c = \frac{TMP}{\mu J} \quad (5)$$

The experimental procedure to get each resistance value, which is listed in Table 3, was as follows: (i) R_m was estimated by measuring the water flux of DI water; (ii) R_t was evaluated by the final flux of activated sludge microfiltration; (iii) the membrane surface was then flushed with water and cleaned with a sponge to remove the cake layer. After that, the DI water flux was measured again to get the resistance of $R_m + R_p$. R_p was calculated from processes (i) and (iii) and R_c from (ii) and (iii). And R_c increases proportionally to the dry cake thickness [19]:

$$R_c = r_c \delta_c \quad (6)$$

r_c is the specific resistance per unit cake thickness, varying with the bulk matrix properties and TMP. The cake thickness was determined by membrane cross-sectional SEM images [20] (see Fig. 3). The r_c values can be easily assessed with cake thickness and cake resistance (Table 3).

3.2.3. Scanning electron microscope

The cake surface and cross-section structure was observed with the help of a scanning electron microscope (SEM) (JEOL JSM-5600LV, Tokyo, Japan). After 24 h, the filtration was stopped and three pieces membrane were cut from the middle of the membrane module for triplicate analysis. The samples were fixed with 3.0% glutaraldehyde in 0.1 M phosphate buffer at pH 7.2. The samples were dehydrated with ethanol, silver-coated by a sputter and observed in the SEM.

3.2.4. Image analysis

The area of each pore in the observed membrane surface was determined using a Leica Q500IW image processing and analysis system (Leica Cambridge Ltd., Cambridge, UK). The distribution of cake pore area was obtained by image analysis.

Images were acquired using SEM are JEPG format coded with True Color (Fig. 4a). Images were transferred to gray-scale formation (256 grey-scale levels) with Adobe Photoshop 7.0 software. Before analyzing an image, a threshold has to be determined in order to distinguish pores from the background, and obtain a binary image (Fig. 4b). For each binary image, threshold was estimated as the grey level value that corresponded to that maximum of the grey level histogram second derivation [21]. The pore area values, a_i, and pore number can be determined by analyzing the binary images. The fractal dimensions were obtained from Eqs. (3) and (4) using image analysis data. The standard deviations for triplicate samples were 1–6%.

4. Results and discussion

4.1. Microfiltration performance: effect of TMP

The effect of TMP on membrane permeate flux is presented in Fig. 5. It was observed that the rate of flux decay

Table 3
A series of resistances and specific resistances during microfiltration of activated sludge with different TMPs

	Items (%)					
	R_m (10^{11} m^{-1})	R_p (10^{11} m^{-1})	R_c (10^{11} m^{-1})	R_t (10^{11} m^{-1})	δ_c (μm)	r_c (10^{16} m^{-2})
40 cm	1.05 (11.5)	1.97 (21.5)	6.14 (67.0)	9.16	21.58	2.85
60 cm	1.05 (7.9)	2.61 (19.7)	9.60 (72.4)	13.26	16.05	5.98
78 cm	1.05 (6.1)	1.92 (11.2)	14.19 (82.7)	17.16	14.96	9.49

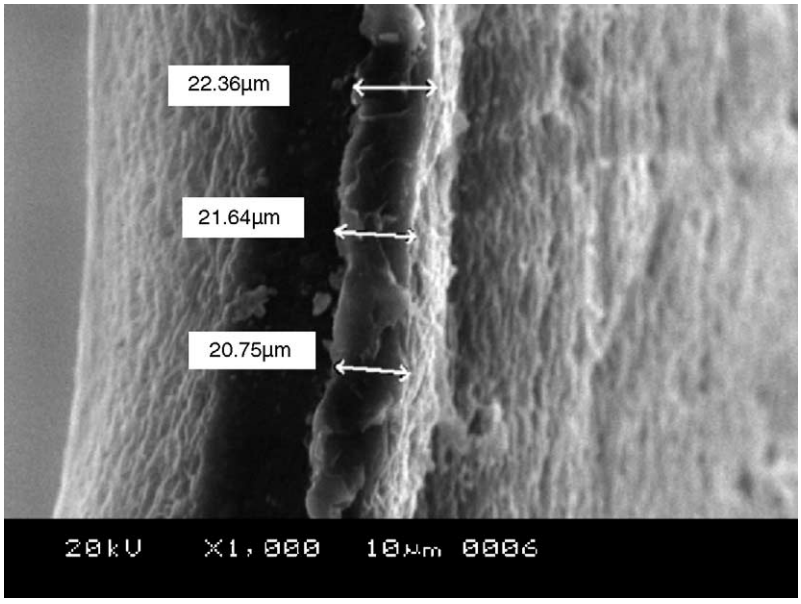

Fig. 3. A side view of cake layer near the membrane surface obtained by SEM (WHD = 40 cm).

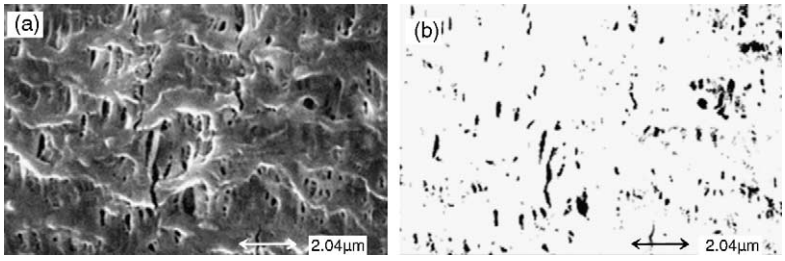

Fig. 4. (a) Initial True Color image; (b) binary image of the cake layer.

increased with increasing TMP, which could be caused by two factors: the thickness of the cake layer and the compactness of the cake layer. At high TMP, more particles accumulated on membrane surface and there was a high drag force resulting in cake compression. Table 3 indicates that membrane cake resistance and specific resistance increased with increasing TMP.

Fig. 5 shows TMP is not only as a driven to membrane filtration, but also an effective factor influence membrane fouling. High TMP will cause faster decline in permeate flux,

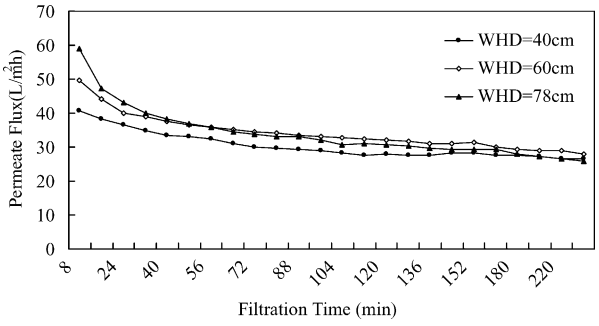

Fig. 5. Effect of TMP on permeate flux of membrane bioreactor.

implying a more compact cake layer formed. Consequently, operating at optimum pressure is a key factor to minimize membrane fouling.

4.2. Comparison of cake layer permeability

To examine the fouling tendencies, each resistance term was calculated (Table 3). As more activated sludge particles were deposited on the membrane surface, the cake resistance increased dramatically and became the dominant resistance. Table 3 indicates that the cake resistance was increased rapidly as TMP increased. The cake resistance of WHD = 78 cm (14.19×10^{11} m^{-1}) was more than two times of WHD = 40 cm, and its proportion increased from 67.0 to 82.7%.

Specific cake resistance is a parameter, which characterizes the physical properties of a cake layer and is in close association with R_c. According to Carman Kozeny relation, the most famous relation for cake filtration implies that for a given particle size, the specific resistance is significantly influenced by cake porosity. The r_c provides an effective method to study membrane fouling mechanism, and it can offer us the compressibility characteristics of microfiltration

Table 4
Results of cake structure analysis

	Items					
	Measured pore count	Minimum pore area (μm^2)	Maximum pore area (μm^2)	Mean pore area (μm^2)	Porosity (%)	D_s
40 cm	1261	0.002	1.056	0.036	7.35	1.9715
60 cm	754	0.002	0.898	0.015	2.58	1.9920
78 cm	515	0.002	0.531	0.021	2.34	1.9925

cake formed by activated sludge particles. For microbial suspensions, the relationship between specific cake resistance and applied pressure can be described by a simple linear equation [22,23]. But there is little research about specific cake resistance on membrane fouling of MBR.

Different methods, including post-mortem measurement and live observation, for cake thickness measurement have been reported in the literature [24]. In our study, the cake thickness was simply examined with SEM images (Fig. 3). The effect of TMP on cake thickness and specific resistance are shown in Table 3. The resulting r_c was determined as $2.85 \times 10^{16}\ m^{-2}$ as WHD = 40 cm, $9.49 \times 10^{16}\ m^{-2}$, for that of WHD = 78 cm. Rapid compression of the cake occurred at higher TMP (WHD = 78 cm) as shown by the significantly higher value of r_c, which was more than three times of WHD = 40 cm. With an increase in TMP, the steady-state cake thickness decreased from 21.58 to 14.96 μm. These results were different from some previous research [24,25]. Vyas et al. [24] during cross-flow microfiltration (CFMF) of lactalbumin particles using a tubular alumina membrane module (0.1 μm pore size, 2.5 mm i.d.) reported that the cake thickness increased with increasing TMP. Wakeman [25] also reported an increase in cake thickness with increasing TMP or with decreasing cross-flow velocity (CFV) during CFMF of calcite and anatase suspensions. In our study, the decrease in the cake thickness was due to an increase in driving force toward the membrane at higher TMP. And cake layer formed by activated sludge is easily compressed. Therefore, the cake thickness with higher TMP may be smaller than lower TMP.

4.3. Fractal analysis of cake layer morphology

In Fig. 6, the SEM images show the surfaces of clean membrane and fouled membrane. New membrane surface is observed to be porous and free of particles (Fig. 6a). The surface of fouled membrane shows the presence of a cake layer (Fig. 6b–d). The size of the cake layers is about 22 μm × 20 μm. The cake layer was seemed to be dense and non-porous. The morphological parameters measured with different TMP are summarized in Table 4 . Observing these SEM images with the data in Table 4 we can clearly understand that the parameters can indeed, to certain degree, quantitatively characterize the cake morphology.

It can be seen that the fouling cake, formed with WHD = 40 cm, had a much higher porosity and a bigger pore diameter than WHD = 60 and 78 cm. The cake pore counts and pore area were decreased as TMP increased. The deposition of activated sludge particles onto the membrane resulted in the formation and maintenance of a relative higher porous cake layer at lower TMP (WHD = 40 cm). Rapid compression

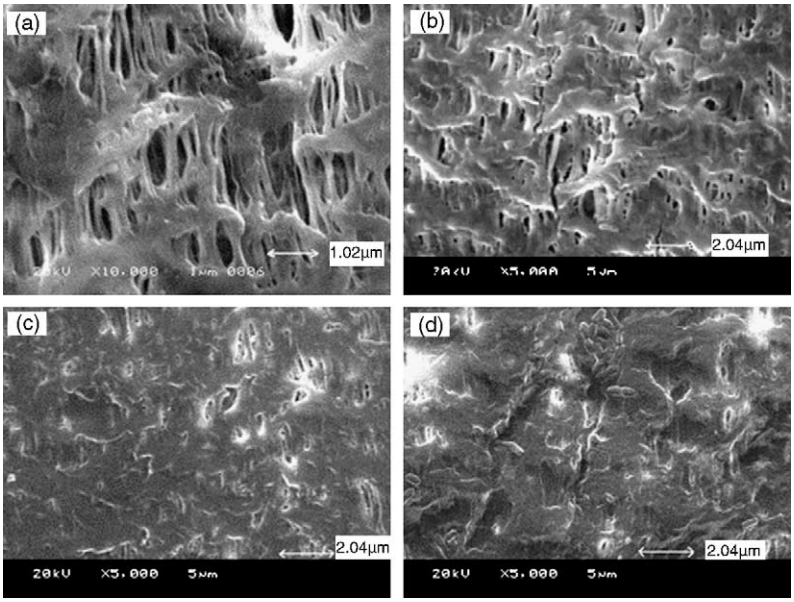

Fig. 6. SEM images showing the surfaces of clean membrane, fouled membrane: (a) new membrane surface; (b), (c) and (d) fouled membrane of WHD = 40, 60 and 78 cm, respectively.

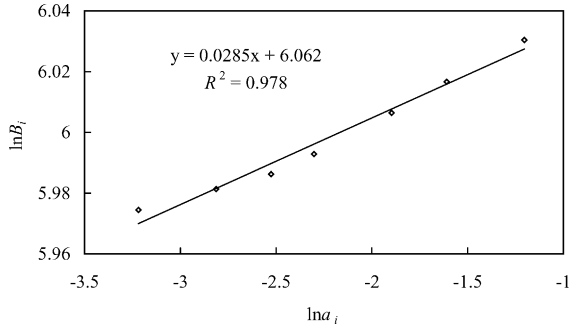

Fig. 7. Determination of fractal dimension (2-slope) plotting double logarithmic of B_i vs. a_i of WHD = 40 cm.

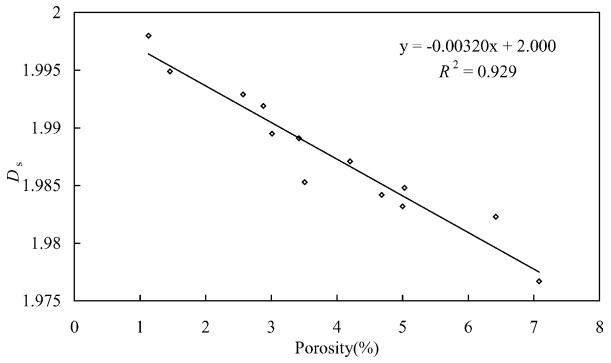

Fig. 8. The relationship between the fractal dimension and the porosity of cake surface.

of the cake occurred at higher TMPs (WHD = 60, 78 cm) as shown by the significantly lower porosity of the cake. Under high TMP conditions, the cake-averaged pore area exhibited a small value.

Analyzing a cake layer SEM image with image analyzer, the overall area of the image S_c was about 440 μm^2. There was a sequence of pores, whose area changed from 0.002 to about 1 μm^2. Several different thresholds of the pore area were determined. Thus A_i and B_i of each level could be easily assessed according to Section 2.2.

A double logarithmic plot of the surplus area, $B_i(\geq a_i)$, and pore area, a_i, of the cake SEM images is shown in Fig. 7. Excellent linearity with high correlation coefficient ($R^2 = 0.978$) was observed, suggesting that the porous structure characterized by the pore area distribution was a typical fractal structure.

The cake permeability is significantly influenced by cake porosity. In order to illuminate the feasibility of fractal theory in our research, several SEM images with different porosity were analyzed. As can be seen from Fig. 8, there was certain linearity between the cake layer porosity and the fractal dimension. It also can be seen that the cake layer would be a two-dimensional plane ($D_s = 2.000$) as its porosity became zero. These results indicate that the fractal dimension of the cake layer surface images can be used directly as a measurable index of the cake layer porosity.

As the WHD increased from 40 to 60 and 78 cm, the fractal dimensions of the cake layers increased from 1.9715 to 1.9920, then increased to 1.9925 (shown in Table 4.). This phenomenon was consistent with the change tendency of porosity. However, cake resistance and cake specific resistance were increased as D_s decreased. It can be seen from Fig. 8 that the cake layer porosity had a good linearity correlation with D_s. According to Carman Kozeny relation, the most famous relation for cake filtration implies that for a given particle size, the specific resistance is significantly influenced by cake porosity. Therefore, there was a close relationship between D_s and cake specific resistance. It implies that the fractal theory can be used to explain the microstructure of cake layer and its formation mechanism. Additionally, it shows that the fractal dimension may be a useful parameter to describe the cake permeability.

5. Conclusions

The microfiltration of activated sludge wastewater is a very complex process, in which membrane fouling is a key problem to be resolved. Cake layer formation can be the dominant membrane fouling mechanisms. The cake layer formed by activated sludge particles is easily compressed. TMP is a dominant factor affecting cake resistance and cake specific resistance. The increase of TMP will lead to cake resistance or specific resistance increased sharply.

The work reported in this paper has shown that careful application of simple techniques, such as SEM and image analysis, can provide a wealth of information about cake layer microstructure. Fractal characteristics were revealed, and research results show that fractal geometry can explain cake properties including cake resistance, cake specific resistance, cake porosity. This work provides a new approach to study membrane fouling cake properties and membrane fouling mechanisms.

Acknowledgements

This work was supported by the National Natural Science Foundation of China through Grant Number 50308004.

References

[1] L. Van Dijk, G.C.G. Roncken, Membrane bioreactors for wastewater treatment: the state of the art and new developments, Water Sci. Tech. 35 (1997) 35–41.
[2] J. Lee, W.-Y. Ahn, C.H. Lee, Comparison of the filtration characteristics between attached and suspended growth microorganisms in submerged membrane bioreactor, Water Res. 35 (2001) 2435–2445.
[3] A.L. Lim, R. Bai, Membrane fouling and cleaning in microfiltrtion of activated sludge wastewater, J. Membr. Sci. 216 (2003) 279–290.
[4] P. Gui, X. Huang, Y. Chen, Y. Qian, Effect of operational parameters on sludge accumulation on membrane surfaces in a submerged membrane bioreactor, Desalination 151 (2002) 185–194.
[5] K.-J. Hwang, C.-L. Hsueh, Dynamic analysis of cake properties in microfiltration of soft colloids, J. Membr. Sci. 214 (2003) 259–273.

[6] T. Tanaka, K.I. Abe, H. Asakawa, H. Yoshida, K. Nakanishi, Filtration characteristics and structure of cake in crossflow filtration of bacterial suspension, J. Ferment. Bioeng. 78 (1994) 455–461.
[7] T. Tanaka, K. Usui, K. Nakanishi, Formation of the gel layer polymers and its effect on the permeation flux in crossflow filtration of *Corynbacterium glutamicum* broth, Sep. Sci. Technol. 33 (1998) 707–722.
[8] K.-J. Hwang, C.-L. Hsueh, A study on the mechanism of cake filtration of soft colloids, in: Proceedings of the 2001 Symposium on Transport Phenomena and its Applications, Taipei, Taiwan, 2001, pp. 19–22.
[9] T.J. Su, J.R. Lu, Z.F. Cui, B.J. Bellhouse, R.K. Thomas, R.K. Heenan, Identification of the location of protein fouling on ceramic membranes under dynamic filtration conditions, J. Membr. Sci. 163 (1999) 265–275.
[10] M. Hamachi, M. Mietton-Peuchot, Analysis of deposit behavior in crossflow microfiltration by means of thickness measurement, J. Chem. Eng. 86 (2002) 251–257.
[11] F. Pignon, A. Magnin, J.M. Piau, B. Cabane, M. Meireles, P. Aimar, P. Lindner, Structural characterization of deposits formed during frontal filtration, J. Membr. Sci. 174 (2000) 189–204.
[12] S. Veerapaneni, M.R. Wiesner, Deposit morphology and head loss development in porous media, Environ. Sci. Technol. 31 (1997) 2738–2744.
[13] B.H. Kaye, Describing filtration dynamics from the prospective fractal geometry, KONA 9 (1991) 48.
[14] X.M. Hu, Q. Luo, C.R. Wang, Investigations on the state of water in a flocculated filter cake, Sep. Sci. Technol. 31 (1996) 1877–1887.
[15] B.B. Mandelbrot, Fractal-form, in: Chance and Dimension, Freeman, San Francisco, 1977 (Chapter 1).
[16] L. Xu, Q.X. Zhu, S.Q. Lu, Study on the cake structure of cross-flow micro-filtration, in: Proceedings the 8th World filtration Congress, London, UK, 2000, p. 449.
[17] X.Y. Xu, J.R. Xu, Y. Kang, Dynamics of air pressure filtration and fractal filter cake constructure, J. Chem. Ind. Eng. 46 (1995) 8–14 (in Chinese).
[18] B.H. Kaye, A random walk through fractal dimensions, Lanrentian, Canada, 1994 (Chapter 6).
[19] F. Greg, M.M. Dermot, M.L. Frank, Modelling the effects of particle polydispersity in crossflow, J. Membr. Sci. 99 (1995) 77–88.
[20] B. Riesmeier, K.H. Kroner, M.R. Kula, Tangential filtration of microbial suspensions: filtration resistances and model development, J. Biotechnol. 12 (1989) 153–172.
[21] C. Cenens, B.K.P. Van, et al., On the development of a novel image analysis technique to distinguish between flocs and filaments in activated sludge images, Water Sci. Technol. 46 (2001) 381–387.
[22] A.A. McCarthy, D.G. O'Shea, N.T. Murray, P.K. Walsh, G. Foley, The effect of cell morphology on the filtration characteristics of the dimorphic yeast *Kluyveromyces marxianus var. marzianus* $NRRL_y2415$, Biotechol. Prog. 14 (1998) 279–285.
[23] A.A. McCarthy, P. Gilboy, P.K. Walsh, G. Foley, Characterisation of cake compressibility in dead-end microfiltration of microbial suspensions, Chem. Eng. Commun. 173 (1999) 79–90.
[24] H.K. Vyas, A.J. Bennett, A.D. Marshall, A new method for estimating cake height and porosity during crossflow filtration of particulate suspensions, J. Membr. Sci. 176 (2000) 113–119.
[25] R.J. Wakeman, Visualisation of cake formation in crossflow microfiltration, Trans. Inst. Chem. Eng. 72 (A) (1994) 530–540.